

A Miniaturized Microbial Fuel Cell with Three-Dimensional Graphene Macroporous Scaffold Anode Demonstrating a Record Power Density of Over 10,000 Wm⁻³ (Electronic supplementary information)

Hao Ren^{1,*}, He Tian^{2,#}, Cameron L. Gardner^{3,†}, Tian-Ling Ren² and Junseok Chae¹

[1] Hao Ren, Prof. Junseok Chae

School of Electrical, Computer and Energy Engineering, Arizona State University, Tempe, AZ 85287 (USA)

*E-mail: hren12@asu.edu

[2] Tian He, Prof. Tian-Ling Ren

Institute of Microelectronics & Tsinghua National Laboratory for Information Science and Technology (TNList), Tsinghua University, Beijing, 10084 (P. R. China)

#Current Address: Ming Hsieh Department of Electrical Engineering, University of Southern California, Los Angeles, CA 90089 (USA)

[3] Cameron L. Gardner

School of Biological and Health Systems Engineering, Arizona State University, Tempe, AZ 85287 (USA)

†Current Address: Department of Genetics, Harvard Medical School, Boston, MA 02115 (USA)

Fabrication of the bare gold current collector

Bare gold current collector fabrication started by mechanically drilling a glass slides with a dimension of 46 mm × 26 mm × 1mm with 6 through holes, one for inlet, one for outlet and four for assembly. Afterwards the glass slide was cleaned by piraha solution and deionized (DI) water. Finally Cr/Au (10nm/200nm) thin film was deposited by magnetic sputtering (Emitech K675XD Turbo Sputter Coater).

Fabrication of the 2D single layer graphene

A 2D single-layer graphene was manufactured by chemical vapor deposition (CVD) on copper foil (25 μm, Alfa Inc.) at 1000 °C. CH₄ and H₂ are utilized for CVD. After CVD, the 2D single layer graphene on copper foil was first spin-coat on polymethyl methacrylate (PMMA). Afterwards, the copper was removed by copper etchant, and it was later cleaned by de-ion water by two times, 30 hours each time and afterwards it was dried for one day. Fig. S-1 illustrates the Raman spectrum of the single layer graphene. Typical G and 2D peak are observed, indicating the single-layer graphene.

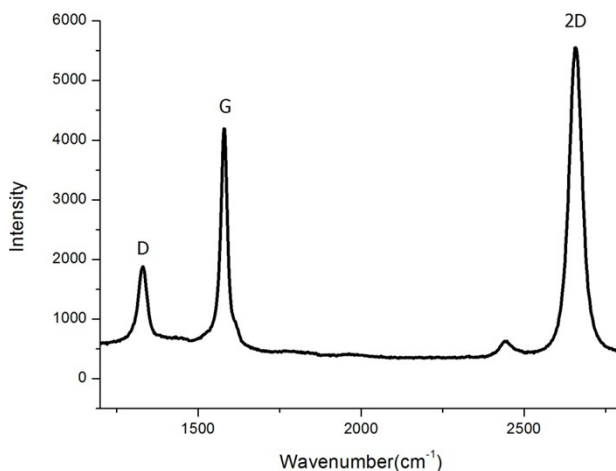


Fig. S-1 Raman spectrum of the single layer graphene

Fabrication of 3D graphene macroporous scaffold

3D graphene macroporous scaffold was prepared by following fabrication procedures which has been described previously¹. Briefly, nickel foams (Alantum Advanced Technology Materials (Shenyang), $\sim 320 \text{ g m}^{-2}$ in areal density and $\sim 1 \text{ mm}$ in thickness) were used as 3D scaffold templates. Graphene was grown by CVD at $1000 \text{ }^\circ\text{C}$. Afterwards, a thin PMMA layer was used as a support to reinforce the graphene scaffold structure for subsequent Nickel foam removal. The Ni foams covered with graphene were drop-coated with a PMMA solution, and then baked at $180 \text{ }^\circ\text{C}$ for 30 min. Then the samples were put into HCl (3 M) solution at 80°C for 3 h to completely dissolve the nickel. Finally free-standing graphene scaffold was obtained by dissolving the PMMA with hot acetone at 55°C . The Raman spectrum of the 3D graphene scaffold is shown in Fig. 1(c), there are two sharp peaks, 2D-band peak at $\sim 2697 \text{ cm}^{-1}$ and G-band peak at $\sim 1581 \text{ cm}^{-1}$. The 2D to G ratio is 0.18, indicating that it is few-layer graphene.

Miniaturized microbial fuel cell (MFC) assembly

The miniaturized MFCs have a PEM (Nafion 117, Sigma Aldrich), to permit cation transport and to avoid electrical short-circuiting. Two silicone gaskets (250 or 500 μm thick, Fuel Cell Store Inc.) are sandwiched between two glass/quartz slides. The cathode is a rectangular glass slide of $2.6 \times 4.6 \text{ cm}^2$ with a layer of Cr/Au or Ti/Pt deposited on top through magnetron sputtering (20nm/200nm) or electron beam evaporation. The anode comprises a glass slide mounted with either single-layer graphene film or 3D graphene scaffold. The size of the electrode is 1 cm^2 . Two nanoports (10-32 Coned assembly, IDEX Health & Science) were used to provide microfluidic pathways into and out of each chamber. The fabrication process of the MFCs started with the preparation of the anodes and cathodes. Then, the nanoports and fluidic tubing (PEEK polymer, IDEX Health & Science) were aligned and glued to the inlets/outlets to supply anolyte and catholyte. Next, silicone rubber gaskets were patterned to define the chamber, electrode, and PEM. Finally, these components were assembled with four screw bolts and nuts to minimize oxygen/electrolyte leakage. Fig. S-2 shows a schematic of the cross-sectional view of the MFC after assembly.

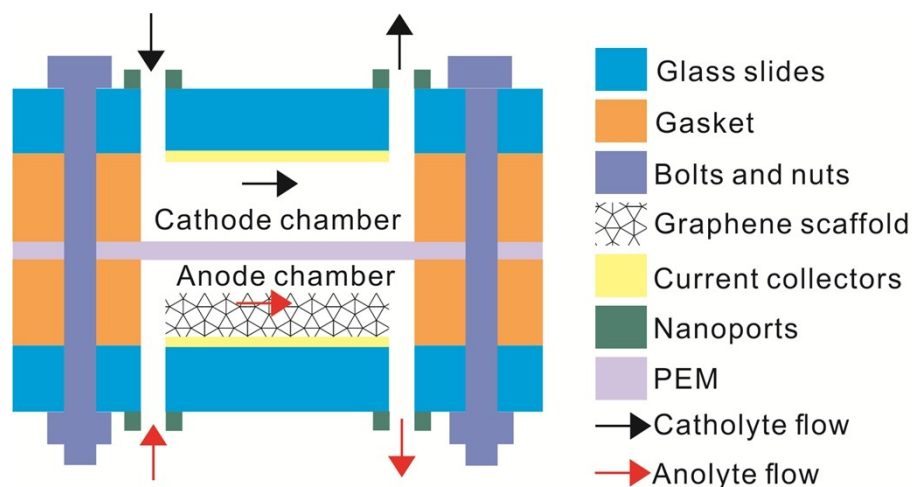


Fig. S-2. cross-sectional view of the miniaturized MFC with 3D graphene anode.

Start-up process of the MFCs

Start-up process of current density versus time for MFCs with variant anodes are shown in Fig. S-3, which is marked by arrows when we performed the polarization of the MFCs. The MFCs with variant anodes were all successfully started up in 7-14 days.

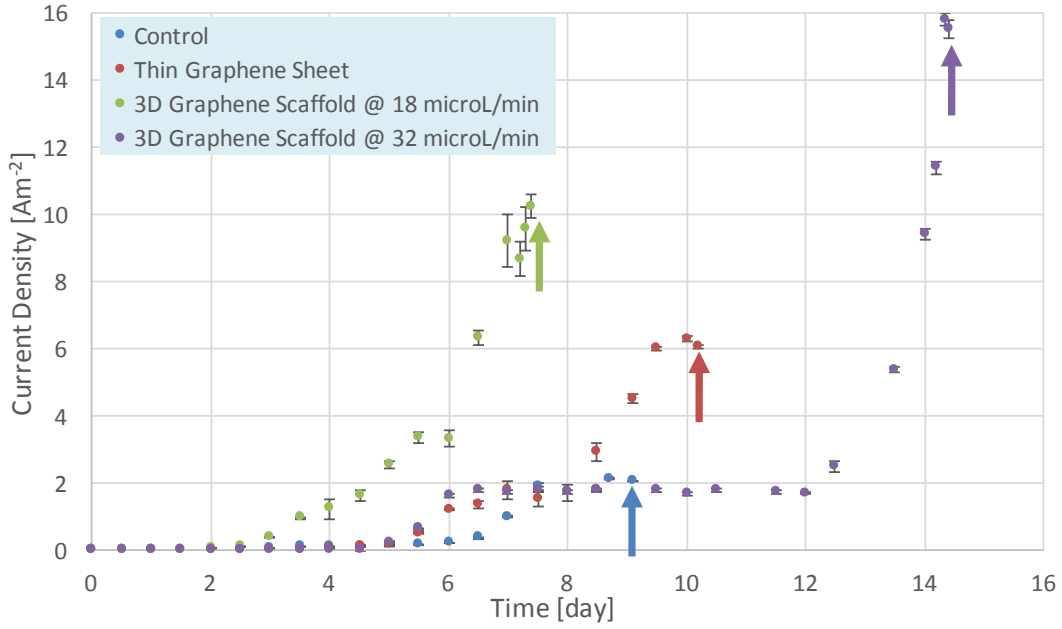


Fig. S-3 Current density profiles over the time of MFCs with different anodes during start-up process

Calculating the density of *Geobacter* on different anodes

The dimension of bacteria is estimated to be 1.5 μm in length and 0.3 μm in diameter, the volume for each *Geobacteraceae* is $v=1.06\times 10^{-19} \text{ m}^3$ ($3.14\times 0.15^2\times 1.5\times 10^{-18}=1.06\times 10^{-19} \text{ m}^3$.) The density of *Geobacter* on different anodes are calculated by equation:

$$d = \frac{A \cdot h}{v} \quad (S - 1)$$

where d is the density of *Geobacter*, A is the projected surface area of anode, and h is the thickness of biofilm.

Quasi-voltammetric curves

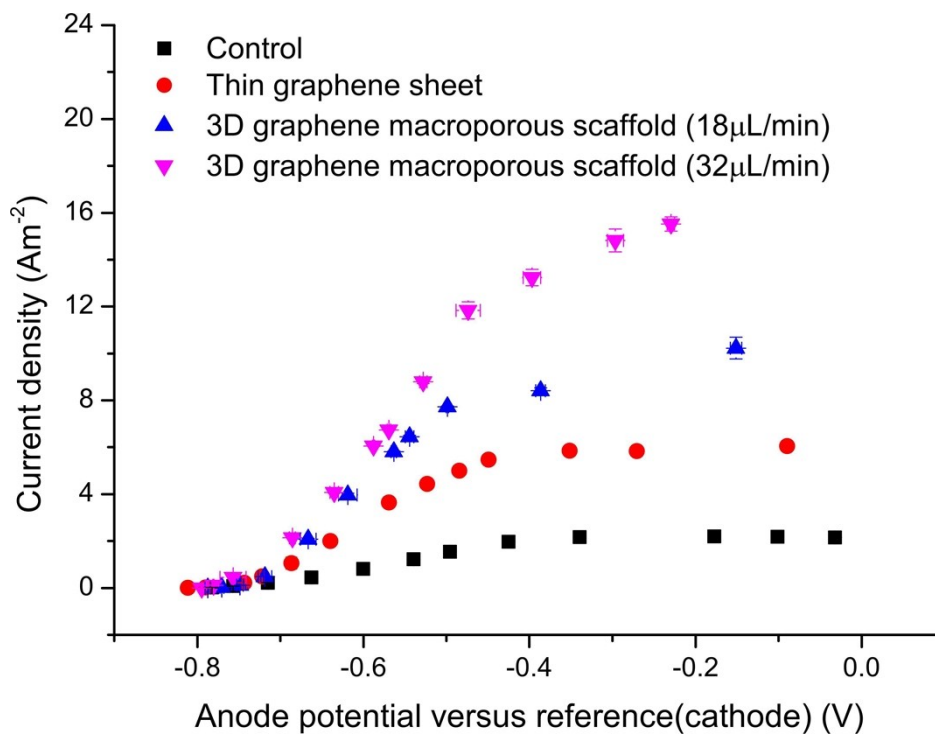


Fig. S-4 Quasi-voltammetric curves of different anodes, presenting 3D graphene scaffold anode marks higher current densities over others at any given potential

The quasi-voltammetric curves of the microbial fuel cell with variant anodes are shown in Fig. S-4. The quasi-voltammetric curve is obtained with two electrodes configuration, thus the anode potential is in reference with cathode potential. The curve shows 3D graphene scaffold anode has the highest current density at any given anode potential among all other electrodes.

A Uni-directional Mass Transfer model

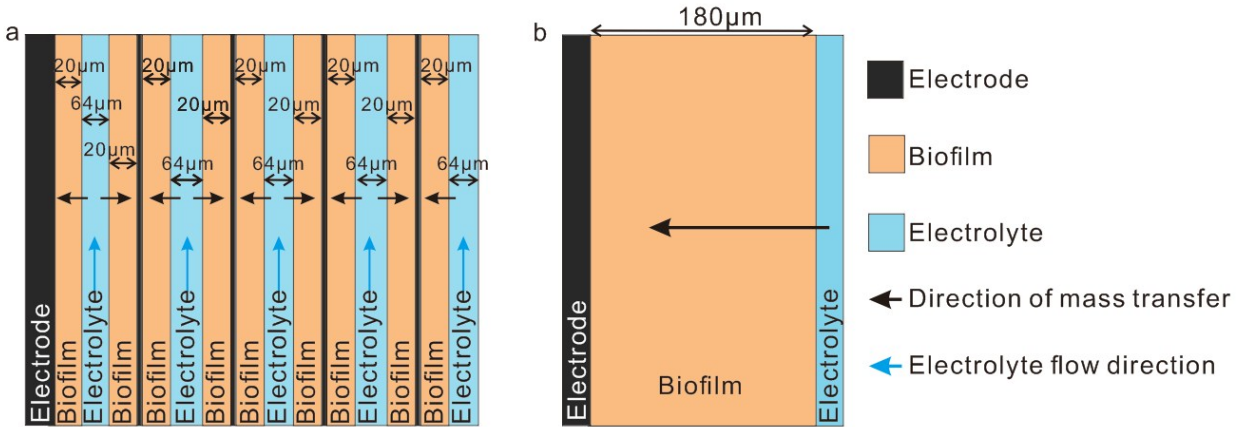


Fig. S-5 Uni-dimensional model of mass transfer inside the biofilm: (a) a stack of biofilms separated by pores that allow electrolyte to flow through and (b) a uniform thick biofilm. Case (a) simulates the 3D macroporous graphene scaffold. According to Fig. 2(b), the biofilm on the 3D graphene scaffold after fixation has a thickness of 150-200 μm , and we assume the thickness of the biofilm to be 180 μm . For simplicity the rest of the chamber height is allocated for the uniform spacing within the stack of biofilm ($(500-180)/5=64 \mu\text{m}$) while case (b) simulates the control group and 2D graphene which have the same thickness with the 3D graphene (in reality, this cannot happen due to the lack of mass transfer, causing severe acidification).

A uni-directional mass transfer model is built, as shown in Fig. S-5. We compare two cases: (a) a stack of biofilms separated by pores that allow electrolyte to flow through, emulating the 3D macroporous graphene scaffold; and (b) a uniform thick biofilm of 180 μm , representing the control group and 2D graphene. The biofilm thickness on the 3D graphene scaffold, after fixation, was measured to be 150-200 μm . Here, we assume 180 μm thick biofilm. For simplicity the rest of 500 μm height chamber is equally distributed between the biofilms. For the uniform thick biofilm, case (b), we assume 180 μm thick biofilm on the electrode.

The time required for the mass transfer of electrolyte into biofilm and be 90% of the bulk electrolyte concentration at the electrode interface can be calculated by Stewart 2003²:

$$t_{90} = 1.03 \frac{L^2}{D_e} \quad (\text{S-2})$$

where L is the thickness of biofilm and D_e is the effective diffusion coefficient in the biofilm.

Taking D_e to be 0.66 cm^2/day (for HPO_4^{2-} , the main buffer³), we can calculate t_{90} as a function of L (Fig. S-6). When L reduces from 180 μm to 20 μm , the t_{90} reduces from 43.7 seconds to 0.54 second. This suggests that the mass transfer improves by a factor of >80, which in return the acidification may be substantially alleviated in (a) over (b). This simple yet effective analytical model concurs that a biofilm having a thickness of 50 μm suffers from acidification that inhibits

the metabolism of *Geobacter surfureducens*⁴. The effective mass transfer is also supported by the experimental data of current density versus flow rate for the 3D graphene scaffold MFC (Fig. S-7).

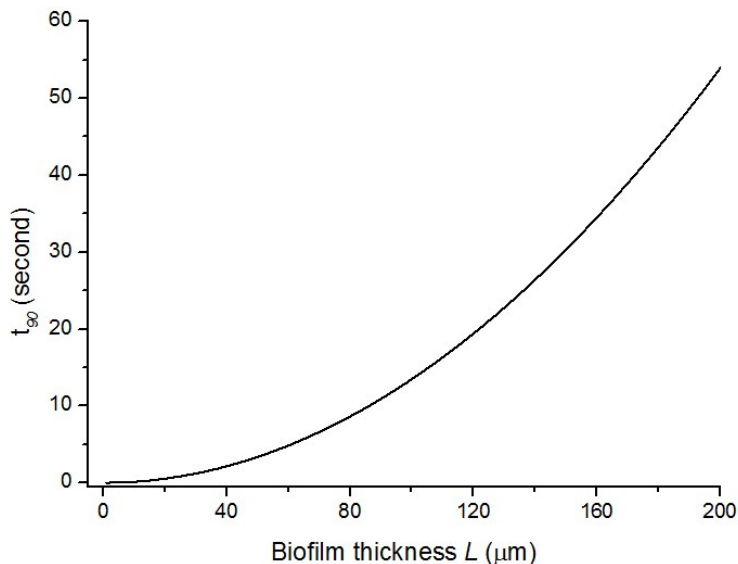


Fig. S-6 t_{90} , the time required for mass transfer of buffer into biofilm and be 90% of the bulk buffer concentration at the electrode interface as a function of biofilm thickness.

The analytical model in Fig. S-5 is supported by the following experimental data. Our prior work (Ren *et al.* 2014) reported the current density is indeed a function of flow rate and mass transfer in microfluidic channel^{5, 6}. The increase of flow rate facilitates the mass transfer in a microfluidic setting to improve the current density, which agrees well with other work reporting the current density is a function of acidification^{3, 4}. According to Ren *et al.* 2014, the flow rate impacts mass transfer coefficient and acidification in a microfluidic setting, thus we can correlate the impact of acidification by characterizing between the flow rate and current density. The flow rate versus current density of our 3D graphene scaffold MFC is shown in Fig. S-7. As flow rate and mass transfer of buffer increases, the current density increases. This suggest the pores inside 3D graphene scaffold allow effective mass transfer, which consequently may alleviate the acidification effect in part, to enhance the current density of MFC.

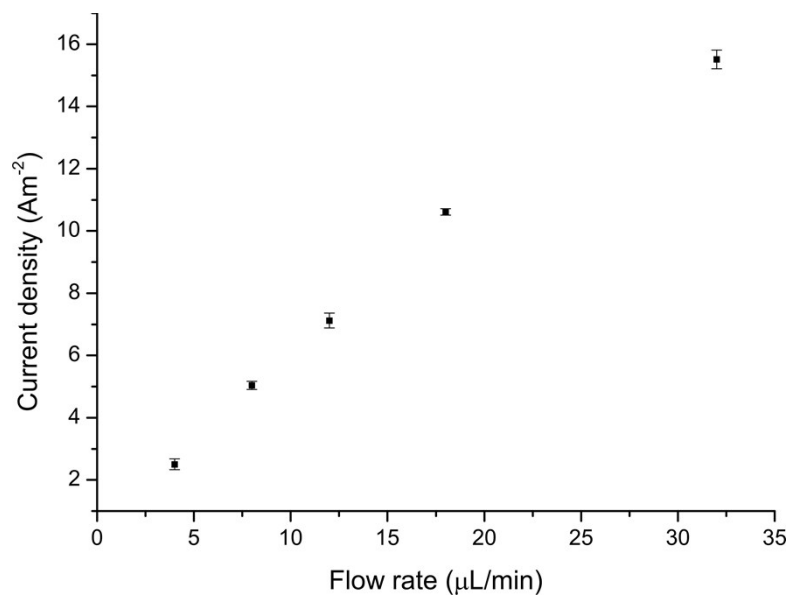


Fig. S-7 Current density versus flow rate of 3D graphene scaffold anode equipped MFC

Coulombic efficiency (CE) measurement

Coulombic efficiency (CE) of the 3D graphene macroporous scaffold MFC was characterized by following the experimental procedure detailed in Ren *et al.* 2014⁸. Briefly, we measured the current versus time profile when we stopped the anolyte supply while keeping the catholyte supply. CE was computed by integrating current profiles over the time and dividing this cumulative charges (C_p) by the charges that could have been produced if all the influent acetate had been oxidized to produce current ($C_T = V \times b \times N_A \times e \times [\text{mol}_{\text{substrate}}]$): $CE = C_p / C_T \times 100 \%$, where V is the volume of anode chamber [m^3], b is the number of moles of electrons produced by oxidation of substrate [8 mol e^- /mol acetate], N_A is Avogadro's number [6.023×10^{23} molecules/mol], e is electron charge [1.6×10^{-19} C/electron], and $\text{mol}_{\text{substrate}}$ is the moles of acetate oxidized.

A high CE of 83% is marked, as illustrated in Fig. S-8, which suggests the successful oxygen mitigation by the MFC setup.

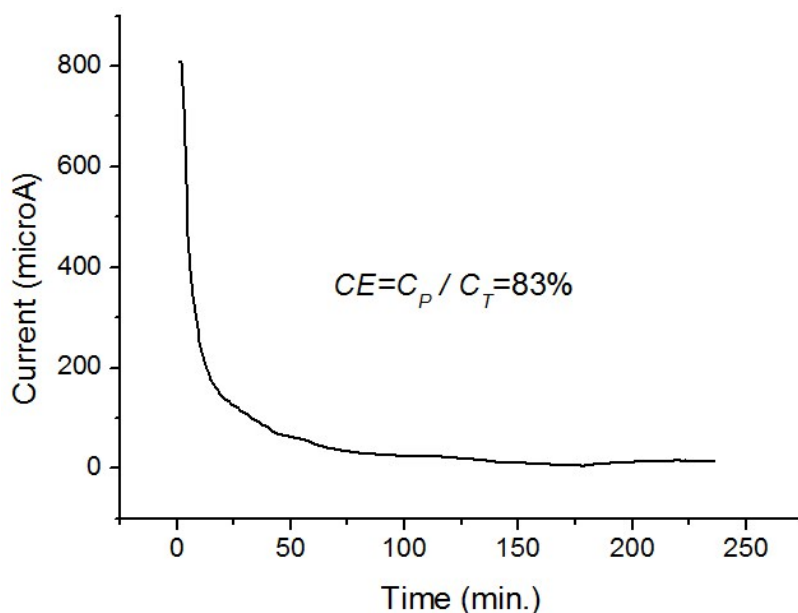


Fig. S-8 Current versus time during the coulombic efficiency (CE) measurement, a high CE of 83% is marked, suggests the successful mitigation of oxygen intrusion.

References

1. Z. Chen, W. Ren, L. Gao, B. Liu, S. Pei and H.-M. Cheng, *Nature materials*, 2011, **10**, 424-428.
2. P. S. Stewart, *J Bacteriol*, 2003, **185**, 1485-1491.
3. C. I. Torres, A. Kato Marcus and B. E. Rittmann, *Biotechnology and Bioengineering*, 2008, **100**, 872-881.
4. A. E. Franks, K. P. Nevin, H. Jia, M. Izallalen, T. L. Woodard and D. R. Lovley, *Energy & Environmental Science*, 2009, **2**, 113-119.
5. H. Ren, C. I. Torres, P. Parameswaran, B. E. Rittmann and J. Chae, *Biosensors and Bioelectronics*, **61** 587-592, 2014.
6. H. Ren, H.-S. Lee and J. Chae, *Microfluidics and Nanofluidics*, 2012, **13**, 353-381.